

Signal Processing on Simplicial Complexes

Feng Ji, Giacomo Kahn, and Wee Peng Tay, *Senior Member, IEEE*

Abstract

Theoretical development and applications of graph signal processing (GSP) have attracted much attention. In classical GSP, the underlying structures are restricted in terms of dimensionality. A graph is a combinatorial object that models binary relations, and it does not directly model complex n -ary relations. One possible high dimensional generalization of graphs are simplicial complexes. They are a step between the constrained case of graphs and the general case of hypergraphs. In this paper, we develop a signal processing framework on simplicial complexes, such that we recover the traditional GSP theory when restricted to signals on graphs. It is worth mentioning that the framework works much more generally, though the focus of the paper is on simplicial complexes. We demonstrate how to perform signal processing with the framework using numerical examples.

Index Terms

Graph signal processing, simplicial complex

I. INTRODUCTION

Many fields of research use data to create hypotheses and try to infer them. Due to this heterogeneous landscape, the data themselves come in diverse forms, from simple binary relations to relations of high arity. One way of incorporating topological properties in data analysis is to use graph signal processing (GSP) [1]–[8]. From signals recorded on networks such as sensor networks, GSP uses graph metrics that relay the topology of the graph to perform sampling, translating and filtering of the signals. Recently, GSP based graph convolution neural network also receives much attention [5], [9]–[11].

GSP, as useful a tool as it is, still has its limitations. The vast data landscape includes complex data, such as high dimensional manifolds, or point clouds possessing high dimensional geometric

The authors are with the School of Electrical and Electronic Engineering, Nanyang Technological University, 639798, Singapore (e-mail: jifeng@ntu.edu.sg, giacomo.kahn@gmail.com, wptay@ntu.edu.sg).

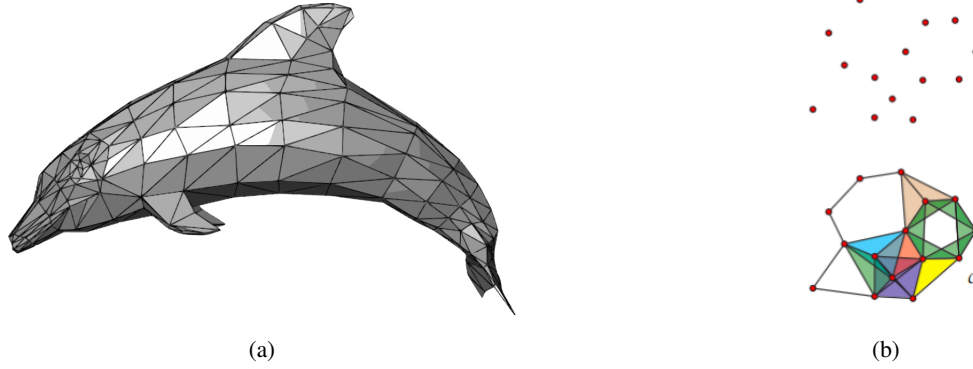


Fig. 1. (a) Approximation of a 2D surface with a 2-complex from Wikimedia Commons. (b) Model of a point cloud (top), together with a simplicial complex (bottom).

features (cf. Figure 1). For example, 2D meshes can be used to approximate a surface and high dimensional simplicial complexes can be used to model discrete point clouds. Another example is in social networks such as Facebook, where an edge represents the friend relation but higher arity edges can represent family links or the inclusion in the same groups. This model also works for group conversations or other user groups in social networks. In addition, some complex interactions cannot be fully grasped by reducing them to binary relations. This is the case with chemical data, where two molecules might interact only in the presence of a third that serves as catalyst [12], [13], or with datasets such as folksonomies, where data are ternary or quaternary relations (users \times ressources \times tag) [14]. Therefore, it is then necessary to go beyond graphs to fully capture these more complex interaction mechanisms.

Moreover, in a lot of applications, a graph learning procedure is involved based on information such as geometric distance, node feature similarity and graph signals [15]–[19]; and due to the lack of definite meaning of edge connections, it is arguable whether a graph is the best geometric object for signal processing. For these reasons, there is a need for a framework that permits signal processing on such high dimensional geometric objects.

Simplicial complexes, as high dimensional generalization of graphs, are independently found in many fields of computer science and mathematics. They are commonly introduced as generalizations of triangles to higher dimensions. Moreover, it is well known that simplicial complexes can be used to model and approximate any reasonable (topological) space according to the *simplicial approximation theorem* [20]. They are already used in topological data analysis [21], representation of surfaces in high dimensions, and modeling of complex networks [22]. In this

paper, we pursue a signal processing framework on simplicial complexes.

Despite the fact that the subject is relatively new, a few attempts have been made. In [23], [24] the authors develop a signal processing framework using a differential operator on simplicial chain complexes. It considers signals associated with high dimensional simplices such as edges and faces, and not only vertices. The paper [25] proposes an approach on meet or join semi-lattices that uses lattice operators as the shift and [26] proposes a framework on hypergraphs using tensor decomposition.

In our paper, we propose another signal processing framework for signals on nodes of simplicial complexes. Our approach makes full use of the geometric structures and strictly generalizes traditional GSP by introducing generalized Laplacians. Signal processing tasks can thus be performed similar to traditional GSP. The rest of the paper is organized as follows. We recall fundamentals of simplicial complexes in Section II. In Section III, we introduce a general way to construct Laplacian on metric spaces, and it is applied simplicial complexes. We focus on the special case of 2-complexes in Section IV. In Section V, we describe the procedure to construct 2-complex structures on a given graph, and discuss how to perform signal processing tasks. We present simulation results in Section VI and conclude in Section VII.

II. SIMPLICIAL COMPLEXES

In this section, we give a brief self-contained overview of the theory of simplicial complexes (see [20], [27] for more details).

Definition 1. *The standard n -simplex (or dimension n simplex) Δ_n is defined as*

$$\{x_0 + \dots + x_n = 1 \mid (x_0, \dots, x_n) \in \mathbb{R}_+^{n+1}\}.$$

Any topological space homeomorphic to the standard n -simplex is called an n -simplex. In Δ_n , if we require $k > 0$ coordinates being 0, we obtain an $(n - k)$ -simplex, called a face.

A simplicial complex X (see Figure 2 for an example) is a set of simplices such that any face from a simplex of X is also in X and the intersection for any two simplices σ_1, σ_2 of X is a face of both σ_1 and σ_2 . A simplex of X is called maximal if it is not the face of any other simplices.

We shall primarily focus on finite simplicial complexes, i.e., a finite set of simplices. The dimension $\dim X$ of X is the largest dimension of a simplex in X . For each $m \geq 0$, the subset of m -simplices of X and their faces is called its m -skeleton, denoted by X^m .

Combinatorially, if we do not want to specify an exact homeomorphism of a n -simplex X with Δ_n , we may just represent it by $n+1$ labels. Therefore, its faces are just subset of the labels. It is worth pointing out that according to the above definition, a simplicial complex is a set of spaces, each homeomorphic to a simplex and they are related to each other by face relations. However, it is possible to produce a concrete geometric object for each simplicial complex.

Definition 2. *The geometric realization of a simplicial complex X is the topological space obtained by gluing simplices with common faces.*

Example 1. *Let X be a finite simplicial complex consisting of two types of simplices E and V . Each simplex in E is 1-dimensional and V contains only 0 simplices. The geometric realization of X is nothing but a graph with vertex set V and edge set E . More generally, for any simplicial complex X , the geometric realization of X^1 is a graph in the usual sense.*

For convenience, we shall not distinguish simplicial complex with its geometric realization when no confusion arises.

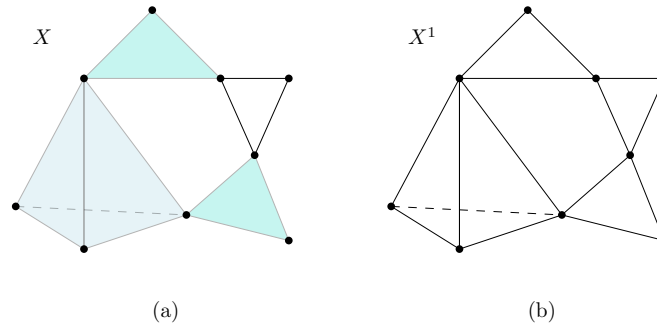


Fig. 2. (a) X is (the geometric realization) of a 3-complex with a maximal 3-simplex, 2 maximal 2-simplices and 3 maximal 1-simplices. (b) X^1 is a connected graph with 15 edges.

In this paper, a simplicial complex X is weighted if X^1 is a weighted graph. Otherwise, we may make an unweighted simplicial complex become weighted by assigning length 1 to each 1-simplex. In this way, X^0 becomes a metric space.

A notion even more general than “simplicial complex” is *hypergraph* [28], [29]. A hypergraph $H = (V, E)$ is a pair where V is a set of vertices and E is a set of non-empty subsets of V , called hyperedges. Each simplicial complex X might be viewed as a hypergraph $H_X = (X^0, E)$, where the vertex set is the 0-skeleton of X and vertices of each simplex of dimension at least 1 give

a hyperedge. Conversely, a hypergraph may not arise from a simplicial complex as such since a subset of a hyperedge might not be a hyperedge, violating the face condition of Definition 1. For each hypergraph H , there is an associated simplicial complex X_H whose simplices are spanned by hyperedges in E as well as their faces. Therefore, the signal processing framework developed in this paper can be directly applied to each hypergraph H , or more precisely, the associated simplicial complex X_H .

III. GENERALIZED LAPLACIAN

Recall that graph signal processing relies heavily on the notion of “shift operator”. A popular choice is the graph Laplacian. In this section, we want to generalize this notion.

Definition 3. *Let X be a finite metric space of size $|X| = n$. A generalized Laplacian consists of the following data:*

- (A) *a weighted, undirected graph $G_X = (V, E)$,*
- (B) *a set function $f : X^0 \rightarrow V$, and*
- (C) *a linear transformation $T : \mathbb{R}^{|X^0|} \rightarrow \mathbb{R}^{|V|}$,*

such that the following holds:

- (a) *f is one-one,*
- (b) *the $f(v)$ component of $T(x)$ is the same as the v component of x for each $v \in X^0$ and $x \in \mathbb{R}^{|X^0|}$, and*
- (c) *the sum of each row of T (written as a transformation matrix) is a constant.*

Let L_{G_X} be the Laplacian of the weighted graph G_X . The generalized Laplacian associated with the data (G_X, f, T) is defined as

$$L_{(G_X, f, T)} = T' \circ L_{G_X} \circ T : \mathbb{R}^{|X^0|} \rightarrow \mathbb{R}^{|X^0|},$$

where T' denotes the adjoint (transpose) of T . We abbreviate $L_{(G_X, f, T)}$ by L_X if no confusion arises from the context.

Intuitively, we require that f is one-one to ensure that f “embeds” X in G_X such that we may perform the shift operation on G_X . Conditions (b) and (c) on T say that the signal on $v \in X^0$ is preserved at its image $f(v)$ in G_X , while signals on $V \setminus f(X)$ are formed from an averaging process.

Lemma 1. (a) L_X is symmetric.

(b) L_X is positive semi-definite.

(c) Constant signals are in the 0 eigenspace of L_X . The 0-eigenspace E_0 of L_X is 1-dimensional if and only if G is connected.

Proof: (a) L_X is symmetric because G_X is assumed to be undirected and hence L_G is symmetric.

(b) Similar to (a), L_X is positive semi-definite because L_{G_X} is positive semi-definite.

(c) As we assume that the sum of each row of T is a constant, therefore if x is a constant vector, then so is $T(x)$. Since constant vectors are in the 0-eigenspace of L_{G_X} , we have $L_{G_X} \circ T(x) = 0$ and so is $L_X(x)$. Therefore, the dimension of E_0 is at least 1.

Now assume that x is in E_0 . Therefore,

$$0 = \langle x, L_X(x) \rangle = \langle T(x), L_{G_X} \circ T(x) \rangle.$$

Consequently, $T(x)$ belongs to the 0-eigenspace of L_{G_X} , which is 1-dimensional if and only if L_G is connected.

By Condition (b), the operator T is injective. Therefore, E_0 is 1-dimensional if and only if $T(E_0)$ is 1-dimensional, which is in turn equivalent to G_X being connected as we just observe. ■

By Lemma 1, the generalized Laplacian L_X enjoys a few desired properties. In particular, being symmetric permits an orthonormal basis consisting of eigenvectors of L_X . Therefore, one can devise a Fourier theory analogous to traditional GSP. Moreover, as L_X is positive semi-definite, we may perform smoothness based learning. The constant vectors belong to the 0-eigenspace is also desirable as it agrees with the intuition that “constant signals are smoothest”.

On the other hand, Lemma 1 asserts that L_X is indeed very similar to the Laplacian of a graph. The theory will be less useful if we are only able to produce weighted graph Laplacian, which we shall prove to be untrue. To this point, we introduce the following notion.

Definition 4. We call L_X graph type if all the diagonal entries of L_X are non-negative and all the off-diagonal entries are non-positive.

Now for simplicial complexes, we are going to give an explicit construction of L_X together with the choice of G, f and T . As an implicit requirement, we would like the construction to recover the usual Laplacian if X is a graph.

For the simplest case, assume $X \cong \Delta_n$ is a weighted n -simplex, i.e., X is homeomorphic to the standard n -simplex and its 1-skeleton X^1 is a weighted graph. We label the vertices of X by v_1, \dots, v_{n+1} . The graph $G_X = (V, E)$ is constructed as follows: $V = \{v_1, \dots, v_{n+1}, u\}$ with a single additional vertex u , which is understood as the barycenter of X . There is no edge between v_i and v_j for any pair $1 \leq i \neq j \leq n+1$. On the other hand, there is an edge connecting v_i and u for each $1 \leq i \leq n+1$.

The edge weight $w(v_i, u)$ between v_i and u is computed as follows:

$$w(v_i, u) = \frac{1}{\binom{n}{2}} \left(\sum_{v_i \neq v_j \neq v_k \neq v_i} (v_j, v_k)_{v_i} \right), \quad (1)$$

where

$$(v_j, v_k)_{v_i} = (d_X(v_i, v_j) + d_X(v_i, v_k) - d_X(v_j, v_k))/2,$$

the Gromov product [30], [31]. Illustrations for $X \cong \Delta_2$ and $X \cong \Delta_3$ are shown in Figure 3.

When $n = 2$, in G_X , we recover pairwise distances between the nodes v_1, v_2 and v_3 in X .

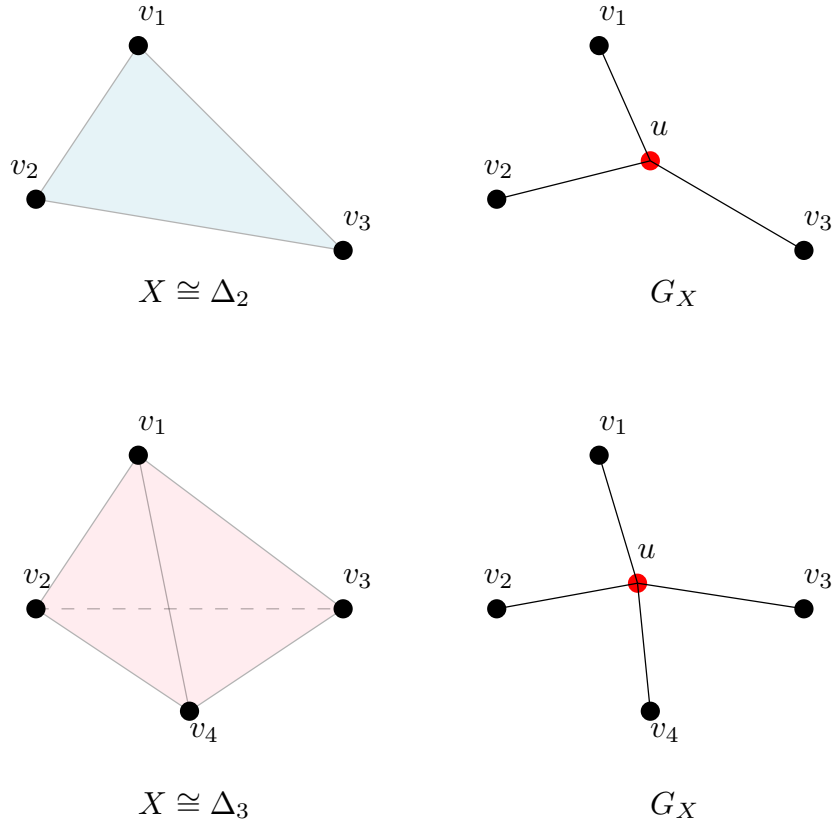


Fig. 3. Graphical illustration of the shape of G_X for $X \cong \Delta_2$ and $X \cong \Delta_3$.

We have a canonical choice for $T: T(v_i) = v_i$. For f , it is identity on each v_i component, while the average is assigned to the u component. In the matrix form,

$$f = \begin{bmatrix} 1 & 0 & \dots & 0 \\ 0 & 1 & \dots & 0 \\ \vdots & \vdots & \ddots & \vdots \\ 0 & 0 & \dots & 1 \\ 1/(n+1) & 1/(n+1) & \dots & 1/(n+1) \end{bmatrix}.$$

It is straightforward to check that (G_X, T, f) verifies the conditions of Definition 3. Thus, we have an associated generalized Laplacian L_X .

For a general finite simplicial complex X , we have a decomposition X^{max} as the subset of the maximal simplices in X and the generalized Laplacian

$$L_X = \sum_{\sigma \in X^{max}} L_\sigma,$$

where the summation is over all maximal simplices of X with appropriate embedding of the vertex indices of σ in X .

To give some insights of the construction, we notice that for $X \cong \Delta_n$, it is topologically (homotopy) equivalent to a point [27]. Therefore, if we want to approximate X by a graph G_X that preserves this topological property, G_X must be a tree. In addition, if we do not want to break the symmetry of the vertices, the most natural step to do so is to add one additional node (the barycenter) connected to every vertex in the original graph. The edge weights of G_X are chosen to approximate the metric of X .

Other evidence for the construction shall be discussed in subsequent sections. We end this section by a discussion when X itself is a graph. In this case, the maximal simplexes are just edges. However, for an edge $e = (v_1, v_2)$ with weight w , the associated graph G_e contains only 3 nodes, v_1, v_2 and an additional node u . Therefore, in this case, Formula (1) no longer applies. On the other hand, to apply Definition 3, we may choose G_X to be X itself and both f and T be the identify map. Therefore, we recover L_X as the usual graph Laplacian.

IV. 2-COMPLEXES

In this section, we focus on 2-complexes, on which the main applications is based on. For a weighted 2-simplex $X \cong \Delta_2$, assume that the edge weights are $w(v_1, v_2)$, $w(v_1, v_3)$ and $w(v_2, v_3)$.

The edge weights of G_X are

$$a = (v_2, v_3)_{v_1} = (w(v_1, v_3) + w(v_1, v_2) - w(v_2, v_3))/2,$$

$$b = (v_1, v_3)_{v_2} = (w(v_2, v_3) + w(v_1, v_2) - w(v_1, v_3))/2,$$

$$c = (v_1, v_2)_{v_3} = (w(v_1, v_3) + w(v_2, v_3) - w(v_1, v_2))/2.$$

If the edge weights satisfy the triangle inequality, then $a \geq 0, b \geq 0, c \geq 0$. Conversely, given $a \geq 0, b \geq 0, c \geq 0$, we are able to recover the edge weights by taking pairwise sums.

The generalized Laplacian L_X is thus given by:

$$\begin{aligned} L_X &= \begin{bmatrix} 1 & 0 & 0 & 1/3 \\ 0 & 1 & 0 & 1/3 \\ 0 & 0 & 1 & 1/3 \end{bmatrix} \begin{bmatrix} a & 0 & 0 & -a \\ 0 & b & 0 & -b \\ 0 & 0 & c & -c \\ -a & -b & -c & a+b+c \end{bmatrix} \begin{bmatrix} 1 & 0 & 0 \\ 0 & 1 & 0 \\ 0 & 0 & 1 \\ 1/3 & 1/3 & 1/3 \end{bmatrix} \\ &= \frac{1}{9} \begin{bmatrix} b+c+4a & c-2a-2b & b-2a-2c \\ c-2a-2b & a+c+4b & a-2b-2c \\ b-2a-2c & a-2b-2c & a+b+4c \end{bmatrix}. \end{aligned}$$

Definition 5. Define the shape constant γ_X of X as

$$\gamma_X = \min\left\{\frac{5w(v_i, v_j) - w(v_i, v_k) - w(v_j, v_k)}{2}, \{i, j, k\} = \{1, 2, 3\}\right\}.$$

In general, γ_X can be negative. This happens when there is at least one very short edge. We use it to address an issue left over from the previous section.

Lemma 2. Suppose $X \cong \Delta_2$ is a 2-simplex. Then L_X is of graph type if and only if $\gamma_X \geq 0$.

Proof: A direct computation shows that

$$-\gamma_X = \max\{c - 2a - 2b, b - 2a - 2c, a - 2b - 2c\}.$$

As the diagonal entries of L_X are all positive, it is of graph type if and only if $-\gamma_X \leq 0$, i.e., $\gamma_X \geq 0$. ■

In the case of 2-simplex, we may also give the following interpretation of L_X with the graph Laplacian L_{X^1} of the 1-skeleton X^1 .

Consider a graph signal $x = (x_1, x_2, x_3)'$ on the vertices $\{v_1, v_2, v_3\}$. Let y be the first order difference $(x_3 - x_2, x_1 - x_3, x_2 - x_1)'$. By a direct computation, one observes that L_X is determined by

$$9\langle x, L_X(x) \rangle = \langle y, L_{X^1}(y) \rangle.$$

It says L_X is a higher order difference, though the point-of-view cannot be generalized beyond dimension 2.

If X is a general 2-dimensional simplicial complex, the Laplacian L_X takes contribution from Laplacian of 2-simplexes computed as above and usual edge Laplacians. We next study spectral properties of L_X . In particular, we want to compare L_X and L_{X^1} as the latter is well-studied. Recall that $A \preceq B$ if $B - A$ is positive semi-definite.

Lemma 3. *Suppose X is a finite 2-dimensional simplicial complex with each edge of length 1. Let k_{\max} and k_{\min} be the largest and smallest numbers of 2-simplexes that share a single edge. Then*

$$\max\left\{\frac{k_{\min}}{3}, \frac{1}{3}\right\} \cdot L_{X^1} \preceq L_X \preceq \frac{k_{\max}}{3} L_{X^1}.$$

Proof: We sketch the main idea of the proof. It suffices to show $L = L_X - \max\{\frac{k_{\min}}{3}, \frac{1}{3}\} \cdot L_{X^1}$ or $L = \frac{k_{\max}}{3} L_{X^1} - L_X$ is the Laplacian of a (possibly disconnected) graph. For this, one only needs to compute the off-diagonal entries of L and show they are non-positive, which follows from direct computation. ■

If X is a 2D-mesh (triangulation) of a compact 2-manifold, then $k_{\min} = 1$ and $k_{\max} = 2$. This is because at most two 2-simplexes can share a common edge and along the boundary each edge is contained in a single 2-simplex.

Recall that a filter F is *shift invariant* w.r.t. L_{X^1} if $F \circ L_{X^1} = L_{X^1} \circ F$. If the graph Laplacian L_{X^1} does not have repeated eigenvalues, then F is shift invariant if and only if $F = P(L_{X^1})$ for some polynomial P of degree at most $n - 1$. The shift invariant family is of particular interest and they are readily estimated as one only has to learn the polynomial coefficients. Due to this fact, L_X will be less interesting if it is shift invariant w.r.t. L_{X^1} , e.g., when X is a single 2-simplex with equal edge weights (more examples are shown in Figure 4). However, this does not happen in general.

Proposition 1. *Suppose X is a 2-complex such that the following condition hold (illustrated in Figure 5):*

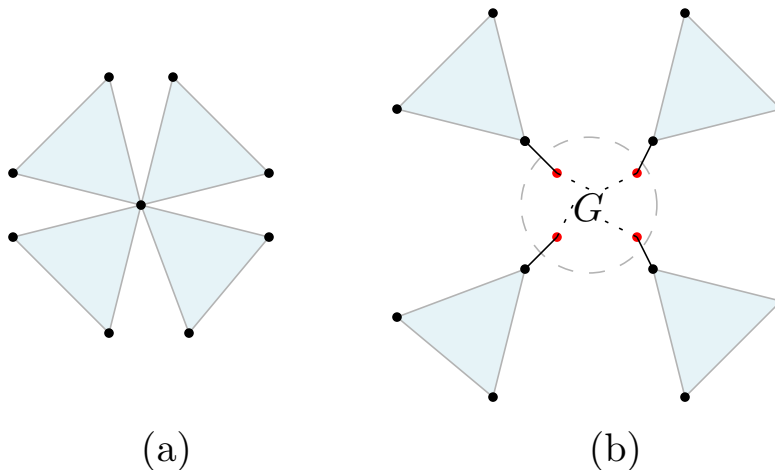


Fig. 4. In (a), if all the edge weights are the same then $L_X = 1/3L_{X^1}$ is shift invariant w.r.t. L_{X^1} . However, in (b), as long as the 4 red nodes are contained in a graph G (at the center), then L_X is not shift invariant w.r.t. L_{X^1} by Proposition 1, even if we allow arbitrary positive edge weights.

(a) In X , any two 2-simplexes are not connected by a direct edge.

(b) In X , if a vertex v is not contained in any 2-simplex, then it is connected to at most one 2-simplex. There is at least one such vertex.

(c) Each edge is contained in at most one 2-simplex.

Then L_X is not shift invariant w.r.t. L_{X^1} .

Proof: The proof is given in Appendix A. ■

V. LEARNING 2-COMPLEX STRUCTURE AND SIGNAL PROCESSING

A. A family of Laplacians

In this section, we discuss the approach to learn a 2-complex structure X given a graph $G = (V, E)$ such that $X^1 = G$ and $X^0 = V$ of size n .

For preparation, if G is an unweighted graph, we assign weight 1 to each edge. Otherwise, if pairwise similarities of V are given, then we define the weight between (v_1, v_2) to be the inverse of the similarity (i.e., we want two nodes to be closer if they are more similar). Therefore, we may assume that $X^1 = G$ is weighted.

The general idea goes as follows. We first identify the set C_{X^0} of all possible 2-simplexes. Depending on the problem, there are two main cases:

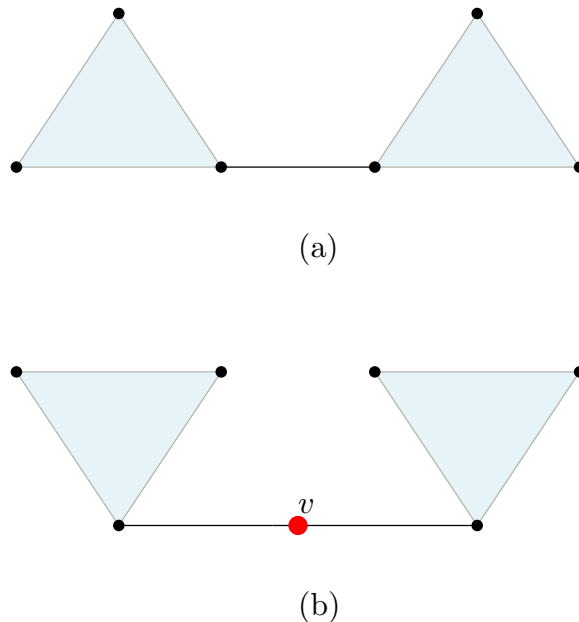


Fig. 5. Illustration of the two situations disallowed by the first two conditions of Proposition 1.

- (a) If $X^1 = G$ is given, then a triple of nodes (v_1, v_2, v_3) belongs to C_{X^0} if and only if (v_1, v_2) , (v_1, v_3) and (v_2, v_3) are all edges of G .
- (b) If only $X^0 = V$ is given, then we assume C_{X^0} contains any triple (v_1, v_2, v_3) of distinct nodes in V .

Given two non-negative numbers $r_1 \leq r_2$, we define $C_{X^0}(r_1, r_2)$ to be the subset of C_{X^0} consisting of triples (v_1, v_2, v_3) whose pairwise edge weights are within the interval $[r_1, r_2]$. Hence, we have the fundamental filtration $\emptyset = C_{X^0}(0, 0) \subset C_{X^0}(0, r) \subset C_{X^0}(0, r') \subset C_{X^0}(0, \infty) = C_{X^0}$ for $r \leq r'$. Next, we perform the following steps:

- (a) Order all the 2-simplices of C_{X^0} in a queue Q :
- (i) Choose $r_0 = 0 \leq r_1 \leq \dots \leq r_m$ such that $C_{X^0} = C_{X^0}(0, r_m)$. A simplex in $C_{X^0}(0, r_i)$ is ordered before that in $C_{X^0}(0, r_{i+1}) \setminus C_{X^0}(0, r_i)$, i.e., small triangles first.
 - (ii) We order the 2-simplices of $C_{X^0}(r_i, r_{i+1})$ in such a way that 2-simplices sharing more edges are ordered later in the queue (with more details given below).
- (b) Partition Q as a disjoint union $Q = \bigcup_{1 \leq i \leq p} Q_i$ such that their sizes are approximately uniform.
- (c) Let X_0 be $X^0 \cup X^1$. For each $1 \leq i \leq p$, we construct a 2-complex X_i by adding the 2-simplices of Q_i (and the associated edges) to X_{i-1} . We form the associated generalized

Laplacians L_{X_i} .

- (d) Approximate the actual Laplacian by using one of L_{X_i} . This step is problem dependent, which in particular relies on the given signal and usually involves an optimization step. We shall be more explicit in Section VI-A.

For completeness, we describe the algorithm for Step (ii) (illustrated in Figure 6):

- (1) For each i , we randomly order the 2-simplexes of Q_i to form Q .
- (2) We want to inductively re-order the members of Q from the initial ordering in Step (1). We start with the first element x_1 of Q . Suppose, for j ranges from the 2-simplexes of Q , we have already ordered x_1, \dots, x_j . Search for the rest of the 2-simplexes of Q . If x is sharing a common edge with x_j , re-order Q by placing x at the end of Q . Once all $x \in Q \setminus \{x_1, \dots, x_j\}$ is gone through once, repeat the procedure for x_{j+1} .

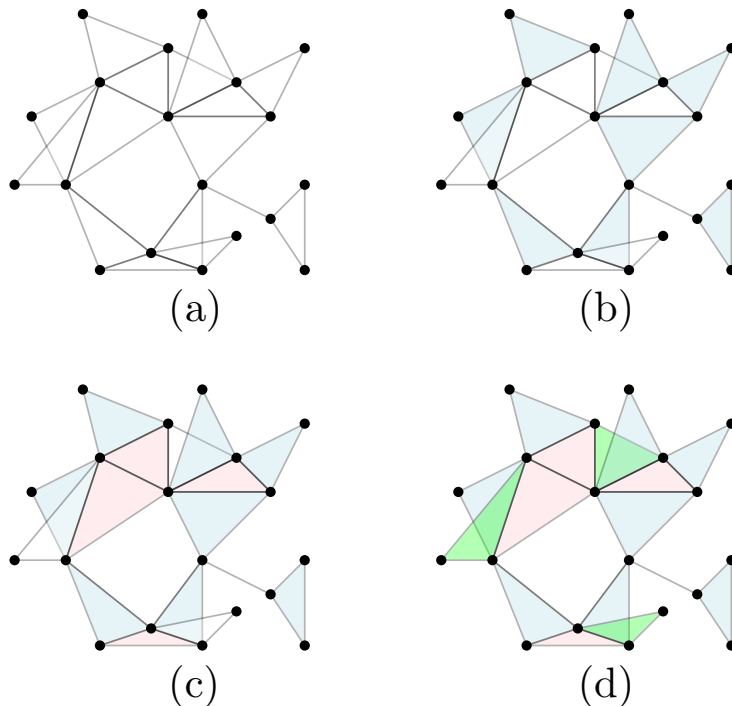


Fig. 6. In this example, the blue 2-simplexes in (b) are (randomly) ordered first in Q . After which, we have the pink 2-simplexes in (c). Finally, the green 2-simplexes are ordered last in Q .

B. Signal processing

With any of L being one of the generalized Laplacian, one may perform signal processing tasks, such as defining Fourier transform, frequency domain, sampling and filtering, similar to

traditional GSP [1], as we now briefly recall:

- (a) Fourier transform: Let $S(V)$ be the space of signals on V and $\{x_i, 1 \leq i \leq n\}$ be an eigenbasis of L . For a signal $x \in S(V)$, its *Fourier transform* is given by

$$\hat{x}(i) = \langle x, x_i \rangle, 1 \leq i \leq n.$$

The inverse transformation is given by:

$$x = \sum_{1 \leq i \leq n} \hat{x}(i)x_i.$$

- (b) Bandlimit and bandpass filters: suppose B is a subset of $\{1, \dots, n\}$. A signal x has *bandlimit* B if $\hat{x}(i) = \langle x, x_i \rangle = 0$ for $i \notin B$. The bandpass filter associated with B is given by $x \mapsto \sum_{i \in B} \hat{x}(i)x_i$. For denoising and data-compression, one may consider bandpass filters associated with B consisting of small indices; while for anomaly detection, one may instead choose B containing large indices.
- (c) Downsampling: if a signal x is bandlimited with B of small size, we can always have full knowledge of x by looking at the signal values at a subset $V_1 \subset V$ of size $|B|$. This is called *downsampling*.
- (d) Convolution: convolution is a generalization of bandpass filters. A convolution kernel is a signal $z \in S(V)$. The associated convolution filter $x \mapsto z * x$ is defined by requiring $\widehat{z * x} = \hat{z}\hat{x}$.
- (e) Shift invariant filters: as we have mentioned earlier, a filter F is shift invariant w.r.t. L if $F \circ L = L \circ F$. If L does not have repeated eigenvalues, a shift invariant filter F is always a polynomial of L .

Remark 1. *Though we do not use it in the paper, it is worth mentioning a continuous filter learning scheme. The basic form of the problem is specified as follows: there are two signals x_1, x_2 on X^0 . Learn the structure of X and an appropriate filter F such that $x_2 = F(x_1) + y$, where y is the white noise.*

For $1 \leq t \leq 1$, let $L_{i,t} = tL_{X_i} + (1-t)L_{X_{i+1}}$. We propose to solve the following optimization problem:

$$\min_{1 \leq i \leq p} \min_{\substack{t \in [0,1] \\ (a_0, \dots, a_b) \in \mathbb{R}^{b+1}}} \left\| \left(\sum_{1 \leq j \leq b} a_j L_{i,t}^j \right) (x_1) - x_2 \right\|^2, \quad (2)$$

where b is a pre-determined bound on the degree of the polynomial. Doing so allows us to get access to the optimal shift $L_{i,t}$ as well as the filter F .

VI. SIMULATION RESULTS

A. Graph learning

In this section, we consider three signal processing tasks: *topology inference*, *signal compression* and *anomaly detection* simultaneously with synthetic experiments.

We start with the Enron email graph G of size $n = 500$ and 6815 pair-wisely connected triples [32]¹. We construct a 2-complex X by randomly adding 2-simplices for pair-wisely connected triples in G . As a result, $G = X^1$ is observed and X is unobserved. Let $B = \{f_1, \dots, f_n\}$ be an eigenbasis of L_X arranged according to increasing order of the associated eigenvalues. We randomly generate a set S_1 of signals from the span of the first $r_1\%$ of base signals.

To learn X from S_1 , we construct X_i and L_{X_i} as in Section IV Step (c) for $0 \leq i \leq p = 20$ where $X_0 = X^1 = G$. Let $V_{r_1,i}$ be the matrix whose columns are the first $r_1\%$ of the eigenvalues of L_{X_i} . Then the estimated simplicial complex X_b and its Laplacian L_{X_b} is obtained by solving the optimization problem:

$$b = \arg \min_{0 \leq i \leq p=20} \sum_{f \in S_1} \|V_{r_1,i} V_{r_1,i}' f - f\|_2^2.$$

The spectrum of L_{X_i} are plotted in Figure 7. In our case, the number of pair-wisely connected triples (6815) is small as compared to the size of the graph (500), as the number of ways choosing 3 nodes among n nodes is of order $O(n^3)$. As a consequence, the triples for our G do not share many common edges. Therefore, as i grows, entries of L_{X_i} tend to have smaller magnitude thus yielding a shift of the spectrum towards 0, as we observed in Figure 7 (c.f. Lemma 3). However, the situation can reverse if a graph is densely connected with a large amount of pair-wisely connected triples. Moreover, we observe that the spectrum pattern more or less stabilize beyond $i = 10$, which suggests that we may choose smaller p as the spectrum stratify the eigenbasis according to smoothness. We make similar observations for other non-dense graphs, e.g. Figure 9.

Now we turn on to performance evaluation. We generate a set S_2 from the first $r_2\%$ ($\leq r_1\%$) of the base signals in B , considered as a set of *compressible signals*. We want to estimate the signal compression error of the estimated Laplacian L_{X_b} as:

$$\text{err} = \sum_{f \in S_2} \|V_{r_2,b} V_{r_2,b}' f - f\|_2.$$

¹<https://snap.stanford.edu/data/email-Enron.html>

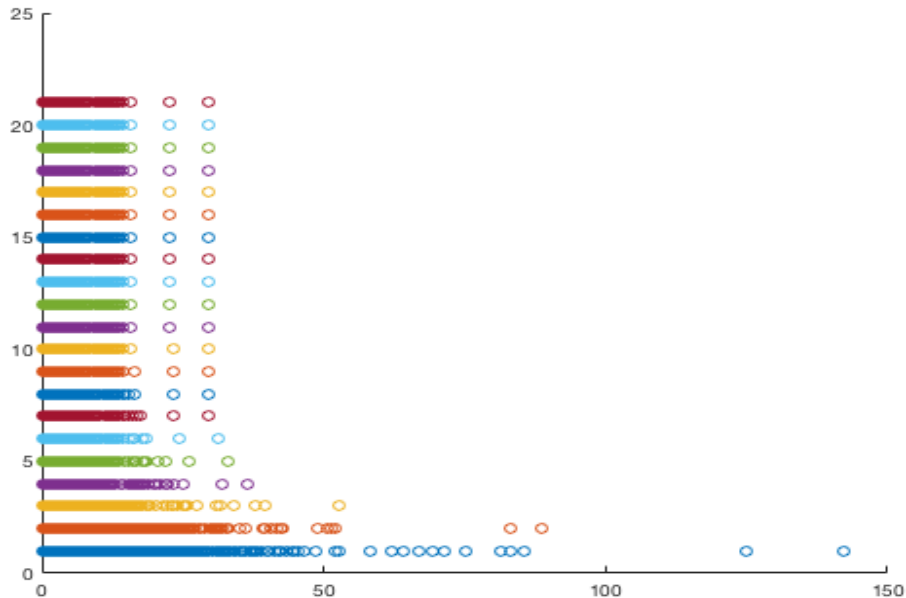


Fig. 7. The plot shows the eigenvalue distribution of $L_{X_0} = L_G$ to $L_{X_{20}}$ from bottom-to-top, for the Enron email graph. The spectrum tends to shift to the left, which might show a “more connected” structure.

For comparison, we perform the same estimation on L_{X_0} , for which we do not consider high dimensional structures. On average for different choices of X , as compared to using L_{X_0} , the compression error with L_{X_b} is reduced by 33.2% and 40.6% for $r_1\% = r_2\% = 30\%$ and 50%, respectively.

Finally, we introduce anomalies to signals in a new set S_3 (with $r_1\% = 2r_2\% = 50\%$) by perturbing the signal value at one random node. We perform spectrum analysis of the anomalous signals using both L_{X_b} and L_{X_0} , again as a comparison between with or without high dimensional structures. Two typical examples of the spectral plots are shown in Figure 8. We see that using L_{X_b} (red), the anomalous behavior is more easily detected by inspecting high frequency portions.

In the subsequent subsections, we shall make more detailed investigation and analysis on anomaly detection and noisy label correction with real datasets.

B. Anomaly detection

The graphs being used in this subsection is a weather station network in US of size 197². The dataset allows us to identify the locations of the weather stations, and the graph G for

²<http://www.ncdc.noaa.gov/data-access/land-based-station-data/station-metadata>

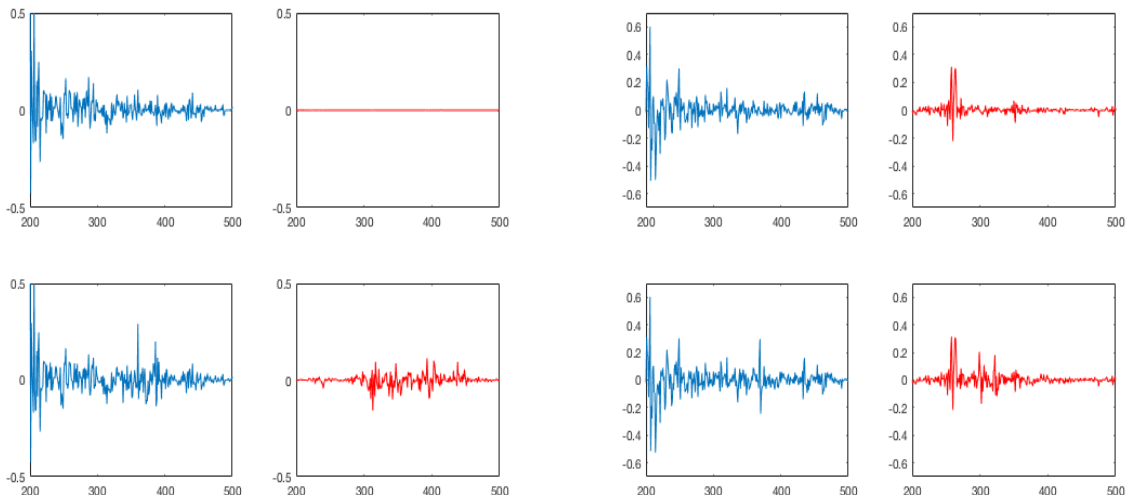


Fig. 8. We have two sets of high frequency component plots. For each set, the left figures (blue) are normal and abnormal plots of L_{X_0} and the right figures (red) are the plots of L_{X_b} . The anomalous behavior is more visible for L_{X_b} .

the weather station network is constructed using the k -nearest neighbor algorithm based on the locations of the stations. The graph G has 495 edges and 395 pair-wisely connected triples.

As in Section VI-A, we construct X_i and L_{X_i} for $0 \leq i \leq p = 20$. The spectrum of L_{X_i} are plotted in Figure 9 with observations similar to those made in Figure 7.

The signals on G_2 are real daily temperature recorded over the year 2013³. For a daily temperature reading x chosen from the one year recording, we introduce anomaly to x by randomly perturbing the value of x at a single node. The resulting signal is denoted by x_a .

As we mentioned in Section VI-A, we may look at the high frequency components of the Fourier transform of x_a , decomposed w.r.t. L_{X_i} for $0 \leq i \leq p$.

The experiment details are given as follows. We fix numbers $0 < r, \epsilon < 1$ and let L be among L_{X_i} . For each instance, we randomly choose a date, and let the temperature signals on the 4 consecutive days starting from the chosen date be x_1, x_2, x_3 and x . The signal x_a is the perturbed version of x . Assume that we only observe the normal signals x_1, x_2, x_3 and the anomalous signal x_a . We perform graph Fourier transform on x_1, x_2, x_3 and x_a to obtain $\hat{x}_1, \hat{x}_2, \hat{x}_3$ and \hat{x}_a . Define

$$a = \max_{j=1,2,3; 197r < k \leq 197} |\hat{x}_j(k)|; b = \max_{197r < k \leq 197} |\hat{x}_a(k)|$$

³<ftp://ftp.ncdc.noaa.gov/pub/data/g sod>

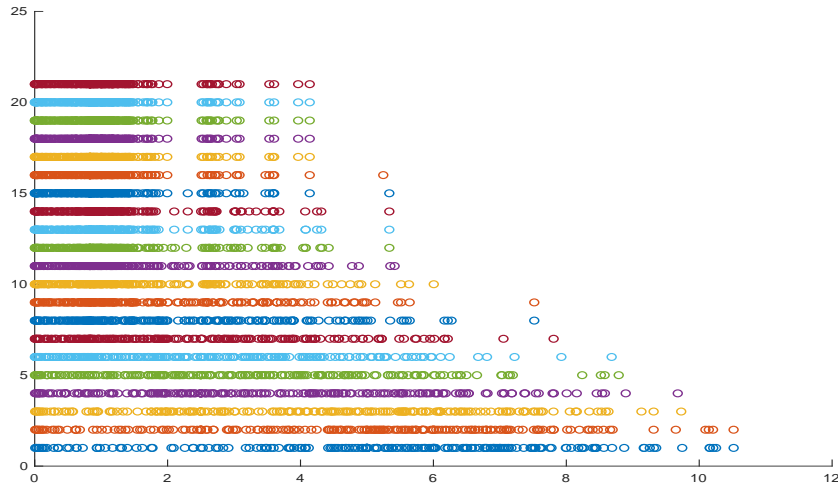


Fig. 9. The plot shows the eigenvalue distribution of $L_{X_0} = L_G$ to $L_{X_{20}}$ from bottom-to-top, for a US weather station network. The spectrum tends to shift to the left, which might show a “more connected” structure.

as a measure of magnitude of the high frequency components of the signals. We declare that x_a is abnormal if $b/a > 1 + \epsilon$.

We run experiments with $r = 0.8$ and $\epsilon = 0.05$. We are interested in the performance in terms of percentage of successful detections under the following circumstances:

- S1. $L = L_{X_0}$, the usual Laplacian for all levels of perturbation.
- S2. The best performance among L_{X_i} for each level of perturbation.
- S3. $L = L_{X_b}$ with the best overall performance for all levels of perturbation ($b = 2$ in our case).
- S4. Anomaly is declared when at least $1/3$ of L_{X_i} , $0 \leq i \leq p$ say so.

The results are summarized in Figure 10. We see that in general, we do gain benefits by working with a simplicial complex instead of a graph. The best simplicial structure is X_2 when approximately 10% of pair-wisely connected triples are added as 2-simplexes. It has a consistent

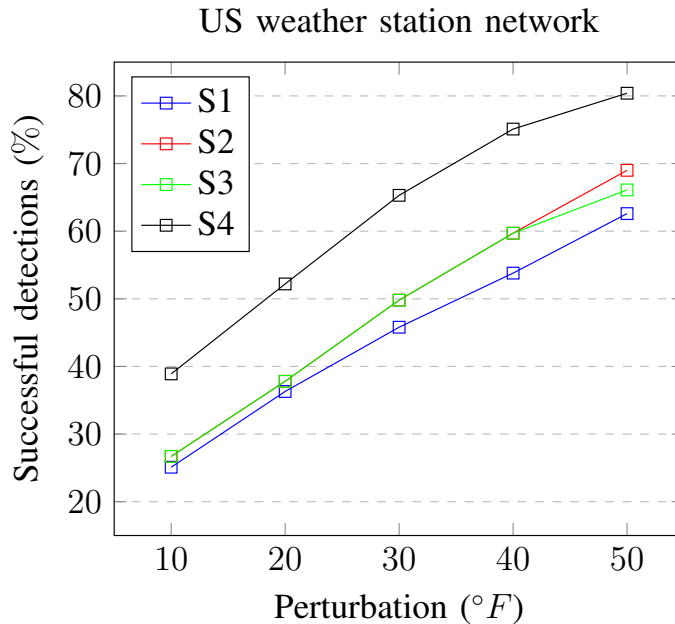


Fig. 10. Performance of anomaly detection on the US weather station network.

overall performance. Moreover, by aggregating observations from different L_{X_i} together, we may further enhance the detection accuracy.

C. Noisy label correction

In this section, we consider noisy label correction with the following experimental setup. On a graph G of size n , suppose every node v belongs to a class among k classes, and thus has a class label $x(v) \in \{1, \dots, k\}$. We assume that a certain percentage of the labels are corrupted by noise. The task is to recover the true label as far as possible.

An approach to the task is to apply a convolution filter to the noisy labels. More specifically, let x_b be the signal of noisy labels and L be a shift operator. Fix a number $0 < r < 1$ and a scaling factor $0 \leq s < 1$. We first find the Fourier transform \hat{x}_b of x_b w.r.t. L . To denoise, we scale down $\hat{x}_b(i)$, $rn \leq i \leq n$ by the factor s to obtain y_b . To obtain the recovered label, we round off the inverse transform of y_b .

The purpose of this paper is to investigate the gain and loss with simplicial complexes over plain graphs. Therefore, we apply the same set of parameters for different choices of L . As in Section VI-A and Section VI-B, we construct X_i and L_{X_i} for $0 \leq i \leq p = 10$. We choose a smaller p as we have seen earlier that the spectrum of L_{X_i} may stabilize quickly.

The graphs we consider are citation graphs: Citeseer (2120 nodes, 3679 edges and 1084 triangles) and Cora (2485 nodes, 5069 edges and 1558 triangles) [10], [33]. We briefly recall that for both graphs each node represents a document, and the label is the category of the document. The edges are citations links, forming the citation graphs.

For each experiment, we add noise to randomly selected 60% of the labels, with a constant signal-to-noise ratio (SNR). We perform denoising with $r = 0.01$ and $s = 0.9$, as suggest by sample frequency plot of x and x_b shown in Figure 11.

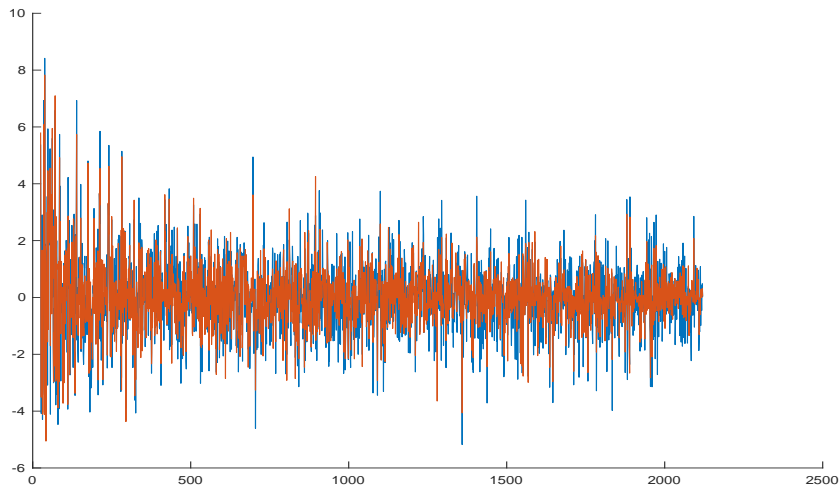


Fig. 11. A sample frequency plot of the actual label x (red) and noisy label x_b (blue) in the range $\approx 0.01n$ to n . We observe fluctuations for both x and x_b , while the amplitudes of x is smaller in general.

In terms of the reducing the amount of error labels, different $L_{X_i}, 0 \leq i \leq p$ perform without noticeable difference. Therefore, for each instance, we determine the L_{X_i} yielding the largest amount of correct labels. Therefore for each i , we can estimate the fraction of instances L_{X_i} being the best. The results are summarized in Table I and II. We highlight three 3 top performers

across each row of the tables.

SNR	L_{X_0}	L_{X_1}	L_{X_2}	L_{X_3}	L_{X_4}	L_{X_5}	L_{X_6}	L_{X_7}	L_{X_8}	L_{X_9}	$L_{X_{10}}$
2	0.127	0.126	0.084	0.105	0.103	0.076	0.086	0.103	0.096	0.046	0.046
1	0.118	0.138	0.076	0.089	0.111	0.088	0.086	0.093	0.100	0.051	0.049
0	0.118	0.131	0.079	0.094	0.114	0.087	0.101	0.099	0.094	0.041	0.041
-1	0.105	0.138	0.093	0.085	0.090	0.093	0.100	0.110	0.098	0.044	0.044
-2	0.127	0.136	0.083	0.093	0.082	0.092	0.094	0.096	0.102	0.047	0.048

TABLE I
CITeseer

SNR	L_{X_0}	L_{X_1}	L_{X_2}	L_{X_3}	L_{X_4}	L_{X_5}	L_{X_6}	L_{X_7}	L_{X_8}	L_{X_9}	$L_{X_{10}}$
2	0.134	0.172	0.099	0.121	0.083	0.084	0.050	0.087	0.060	0.051	0.060
1	0.143	0.163	0.063	0.126	0.125	0.063	0.083	0.094	0.053	0.040	0.048
0	0.115	0.133	0.101	0.085	0.103	0.129	0.077	0.041	0.051	0.070	0.091
-1	0.136	0.134	0.085	0.127	0.049	0.093	0.088	0.056	0.046	0.066	0.120
-2	0.124	0.093	0.132	0.153	0.089	0.078	0.042	0.059	0.076	0.089	0.065

TABLE II
CORa

From the results, we observe that L_{X_1} has the best overall performance consistently, which is when approximately 10% of pair-wisely connected triples are added as 2-simplexes. As a general trend, the perform drops if a large amount of 2-simplexes are added as in X_9 and X_{10} . We do gain benefits by working with high dimensional components against the plain graphs.

VII. CONCLUSIONS

In this paper, we have proposed a signal processing framework for signals on simplicial complexes. To do so, we introduced a general way to construct a Laplacian matrix on a space, which may not be a graph. After which, signal processing follows in the way similar to traditional GSP. We test the framework with both synthetic and real datasets, and observe that we do gain benefits by working with additional high structures.

A lot of new signal processing techniques and problems may stem from our new framework. For future works, we shall exploring such possibilities including continuous filter estimation and data driven based end-to-end learning.

APPENDIX A
NON SHIFT INVARIANCE

In this appendix, we assume X is a 2-complex of size n and discuss conditions that ensure L_X is not shift invariant w.r.t. L_{X^1} . We are mainly interested in geometric conditions, which can be observed directly from the shape of X . As a corollary, we prove Proposition 1. Most of the notations follow those defined in Section IV.

For convenience, we introduce the following notion.

Definition 6. *If a matrix M is the Laplacian of a weighted graph G , then we say M is of graph type G . Moreover, we say that X has distinctive 2-simplexes if (a) either $L_X - L_{X^1}$ or $L_{X^1} - L_X$ is of graph type G ; and (b) an edge $e = (v_1, v_2)$ of G has positive edge weights when e belongs to a 2-simplex of X .*

Lemma 4. *X has distinctive 2-simplexes if either of the following holds:*

- (a) $k_{\max} \leq 1$, i.e., each edge is contained in at most one 2-simplex.
- (b) $k_{\max} \leq 2$ and all the edges have weight 1.
- (c) $k_{\min} \geq 4$ and all the edges have weight 1.

Proof: (a) As any constant vector is in the kernel of $L = L_{X^1} - L_X$, the sum of each row is 0. If (i, j) is an edge of X not contained in any 2-simplex, then the (i, j) -th entry of L is 0. It suffices to show that if (v_i, v_j) is any edge contained in a 2-simplex, then the (i, j) -th entry of L is negative. Let $a > 0$ be the weight of (v_i, v_j) and $b > 0, c > 0$ be the weights of the other two edges of the 2-simplex containing (v_i, v_j) . A direct calculation shows that the (i, j) -th entry of L is $-(13a + b + c)/18 < 0$.

(b) and (c) can be shown by the same argument by considering $L_{X^1} - L_X$ and $L_X - L_{X^1}$ respectively. ■

Assume for the rest of this appendix that X has distinctive 2-simplexes. We want to study common eigenvectors of both L_{X^1} and L_X . To this end, we divide the discussion into two parts: for such an eigenvector, whether the associated eigenvalues are the same or different.

Definition 7. *We call a vertex v is 1-interior if it is not contained in any 2-simplex and 2-interior if each edge containing v belongs to a 2-simplex (see Figure 12 for an example).*

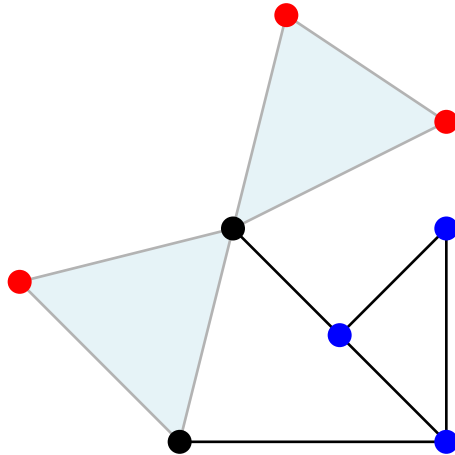


Fig. 12. In this example, all the blue nodes are 1-interior and red nodes are 2-interior. Hence, for the parameters in Lemma 5(b) $m_1 = 3$ and $m_2 = m_3 = 1$. Moreover, in Lemma 6(b), $m_4 = 2$ counts the two black nodes.

Lemma 5. (a) *Let K be the vector space spanned by common eigenvectors with the same eigenvalue of L_X and L_{X^1} . Then K is a subspace of $\ker(L_X - L_{X^1})$.*

(b) *Let m_1 be the number of 1-interior nodes of X , m_2 be the number of connected components of smallest complex containing all the 2-simplices of X , and m_3 be the number of such components containing some 2-interior nodes. Then $\dim K \leq m_1 + m_2 - m_3$.*

Proof: (a) As we assume that X has distinctive 2-simplices, $L_{X^1} - L_X = L_G$ or $-L_G$ for some graph G whose positive edge weights are supported on 2-simplices of X . Therefore, if w is a common eigenvector with the same eigenvalue, then $L_G(w) = 0$, i.e., $w \in \ker(L_G)$. As $\ker(L_G)$ is a vector space, K as spanned by these w 's is also contained in $\ker(L_G)$.

(b) Notice that $\ker(L_G)$ is the same as the number of connected components of G . The set of connected components of G consists of: (1) each 1-interior node of X is an isolated component of G , (2) a union of 2-simplices that is connected. They are of size m_1 and m_2 respectively. Suppose a component C of the second type contains a 2-interior node v and w is a common eigenvector with the same eigenvalue $\lambda > 0$. Then $L_{X^1}(w)(v) = L_G(w)(v) = 0$. However, $L_{X^1}(w)(v) = \lambda w(v)$, and hence $w(v) = 0$. Hence, w is 0 on all of C as w is constant on C . Hence, the vectors of K vanishes on such a C . Therefore, $\dim K \leq m_1 + m_2 - m_3$. ■

Now we consider common eigenvectors of L_{X^1} and L_X with different eigenvalues.

Lemma 6. *Suppose w is a common eigenvectors of L_{X^1} and L_X with different eigenvalues.*

Then

- (a) w is 0 at 1-interior nodes of X .
- (b) If v belongs to a 2-simplex and any 1-interior neighbor of v is not connected to any other node belonging to a 2-simplex, then w is 0 at v . Denote the number of such vertices by m_4 .

Proof: Suppose the eigenvalues of w are $\lambda_1 \neq \lambda_2$.

(a) Let v be a 1-interior node. Then $L_X(w)(v) = L_{X^1}(w)(v)$ as the neighborhood of v in X and X^1 are identical. This implies that $\lambda_1 w(v) = \lambda_2 w(v)$. This is possible only if $w(v) = 0$.

(b) Let v' be a 1-interior neighbor of v . By (a), $w(v') = 0$. As v' is not connected to any other node belonging to a 2-simplex, w is 0 at the neighbors of v' except at v . Hence $0 = L_{X^1}(w)(v') = aw(v)$, where a is the positive edge weight between v and v' . This proves (b). ■

Now, we are ready to state and prove the main result of this section.

Theorem 1. *If $\dim K \leq m_1 + m_4 < n$, then there does not exist any orthonormal basis consisting of common eigenvectors of both L_{X^1} and L_X . In particular, this holds if $m_2 \leq m_3 + m_4$.*

Proof: Suppose on the contrary that $W = \{w_1, \dots, w_n\}$ (column vectors) is an orthonormal basis consisting of common eigenvectors of L_{X^1} and L_X . There are at most $\dim K$ vectors of W each shares the same eigenvalue. Without loss of generality, assume they are $\{w_1, \dots, w_{\dim K}\}$ and let w_1 be the constant vector $(1/\sqrt{n}, \dots, 1/\sqrt{n})'$. Moreover, by re-indexing, we further assume that the first $m_1 + m_4$ indices correspond to the set S of 1-interior nodes and nodes satisfy Lemma 6(b).

By abuse of notation, write W for the $n \times n$ matrix whose i -th column being w_i . As the columns of W forms a orthonormal basis, so do the rows of W . On the other hand, by Lemma 6, only the leading $(m_1 + m_4) \times \dim K$ block W_1 of the first $m_1 + m_4$ rows of W can contain non-zero entries. Hence, the rows of W_1 forms an orthonormal system. This shows that $m_1 + m_4 \leq \dim K$.

We claim $m_1 + m_4 \neq \dim K$. For otherwise, W_S is a $\dim K \times \dim K$ matrix with orthonormal rows. Hence, the columns of W_S also forms an orthonormal system. However, this is impossible as the norm of the first column of W_S is $\dim K/n < 1$.

Therefore, we have shown that $m_1 + m_4 < \dim K$ with the existence of W . This contradicts the assumption that $\dim K \leq m_1 + m_4$. Furthermore, the condition $m_2 \leq m_3 + m_4$ implies that $\dim K \leq m_1 + m_4$ by Lemma 5(b). ■

As a corollary, we can prove Proposition 1 by counting. First of all, by Condition (c), X has distinctive 2-simplexes. In order to show L_X is not shift invariant w.r.t. L_{X^1} , we want to prove that they cannot have a common orthonormal eigenbasis. By Theorem 1, it suffices to show that $m_2 \leq m_4$ under the assumptions of Theorem 1. Let C be a union of 2-simplexes contributing 1 to m_2 in X . In C , there is at least one vertex v_C connected to a 1-interior point for otherwise, we can either add another 2-simplex to enlarge C or X contains no 1-interior point, which contradicts Condition (b). Moreover, v_C cannot be shared by another connected union of 2-simplexes by Condition (a). In conclusion, $C \mapsto v_C$ is a one-one map and hence $m_2 \leq m_4$, and Proposition 1 follows.

REFERENCES

- [1] D. I. Shuman, S. K. Narang, P. Frossard, A. Ortega, and P. Vandergheynst, “The emerging field of signal processing on graphs: Extending high-dimensional data analysis to networks and other irregular domains,” *IEEE Signal Process. Mag.*, vol. 30, no. 3, pp. 83–98, May 2013.
- [2] A. Sandryhaila and J. M. F. Moura, “Discrete signal processing on graphs,” *IEEE Trans. Signal Process.*, vol. 61, no. 7, pp. 1644–1656, April 2013.
- [3] —, “Big data analysis with signal processing on graphs: Representation and processing of massive data sets with irregular structure,” *IEEE Signal Process. Mag.*, vol. 31, no. 5, pp. 80–90, Sept 2014.
- [4] X. Dong, D. Thanou, P. Frossard, and P. Vandergheynst, “Learning laplacian matrix in smooth graph signal representations,” *IEEE Transactions on Signal Processing*, vol. 64, no. 23, pp. 6160–6173, 2016.
- [5] H. E. Egilmez, E. Pavez, and A. Ortega, “Graph learning from data under laplacian and structural constraints,” *IEEE Journal of Selected Topics in Signal Processing*, vol. 11, no. 6, pp. 825–841, 2017.
- [6] F. Grassi, A. Loukas, N. Perraudin, and B. Ricaud, “A time-vertex signal processing framework: Scalable processing and meaningful representations for time-series on graphs,” *IEEE Trans. Signal Process.*, vol. 66, no. 3, pp. 817–829, Feb 2018.
- [7] A. Ortega, P. Frossard, J. Kovačević, J. M. Moura, and P. Vandergheynst, “Graph signal processing: Overview, challenges, and applications,” *Proceedings of the IEEE*, vol. 106, no. 5, pp. 808–828, 2018.
- [8] F. Ji and W. P. Tay, “A Hilbert space theory of generalized graph signal processing,” *IEEE Trans. Signal Process.*, vol. 67, no. 24, pp. 6188 – 6203, Dec. 2019.
- [9] M. Defferrard, X. Bresson, and P. Vandergheynst, “Convolutional neural networks on graphs with fast localized spectral filtering,” in *Advances in Neural Inform. Process. Syst.*, USA, 2016, pp. 3844–3852.
- [10] T. N. Kipf and M. Welling, “Semi-supervised classification with graph convolutional networks,” *arXiv preprint arXiv:1609.02907*, 2016.
- [11] R. Li, S. Wang, F. Zhu, and J. Huang, “Adaptive graph convolutional neural networks,” in *Thirty-second AAAI conference on artificial intelligence*, 2018.
- [12] S. Klamt, U.-U. Haus, and F. Theis, “Hypergraphs and cellular networks,” *PLoS computational biology*, vol. 5, no. 5, p. e1000385, 2009.
- [13] C. Flamm, B. M. Stadler, and P. F. Stadler, “Generalized topologies: hypergraphs, chemical reactions, and biological evolution,” in *Advances in Mathematical Chemistry and Applications*. Elsevier, 2015, pp. 300–328.

- [14] S. Lohmann and P. Díaz, “Representing and visualizing folksonomies as graphs: a reference model,” in *Proceedings of the International Working Conference on Advanced Visual Interfaces*, 2012, pp. 729–732.
- [15] N. Altman, “An introduction to kernel and nearest-neighbor nonparametric regression.”
- [16] X. Dong, D. Thanou, M. Rabbat, and P. Frossard, “Learning graphs from data: A signal representation perspective,” *IEEE Signal Process. Mag.*, vol. 36, no. 3, pp. 44–63, 2019.
- [17] G. Mateos, S. Segarra, A. G. Marques, and A. Ribeiro, “Connecting the dots: Identifying network structure via graph signal processing,” *IEEE Signal Process. Mag.*, vol. 36, no. 3, pp. 16–43, 2019.
- [18] M. Ramezani-Mayiami, M. Hajimirsadeghi, K. Skretting, R. S. Blum, and H. Vincent Poor, “Graph topology learning and signal recovery via bayesian inference,” in *2019 IEEE Data Science Workshop (DSW)*, 2019, pp. 52–56.
- [19] F. Ji, W. Tang, W. P. Tay, and E. K. P. Chong, “Network topology inference using information cascades with limited statistical knowledge,” *Information and Inference: A Journal of the IMA*, 2020.
- [20] E. H. Spanier, *Algebraic topology*. Springer Science & Business Media, 1989.
- [21] G. Carlsson, “Topology and data,” *Bulletin of the American Mathematical Society*, vol. 46, no. 2, pp. 255–308, 2009.
- [22] O. T. Courtney and G. Bianconi, “Generalized network structures: The configuration model and the canonical ensemble of simplicial complexes,” *Phys. Rev. E*, vol. 93, p. 062311, Jun 2016.
- [23] S. Barbarossa and S. Sardellitti, “Topological signal processing over simplicial complexes,” *arXiv preprint arXiv:1907.11577*, 2019.
- [24] S. Barbarossa and M. Tsitsvero, “An introduction to hypergraph signal processing,” in *EEE Int. Conf. Acoustics, Speech and Signal Process.*, 2016, pp. 6425–6429.
- [25] M. Puschel, “A discrete signal processing framework for meet/join lattices with applications to hypergraphs and trees,” in *IEEE Int. Conf. Acoustics, Speech and Signal Process.*, 2019, pp. 5371–5375.
- [26] S. Zhang, Z. Ding, and S. Cui, “Introducing hypergraph signal processing: theoretical foundation and practical applications,” *arXiv preprint arXiv:1907.09203*, 2019.
- [27] A. Hatcher, *Algebraic Topology*. Cambridge University Press, 2002.
- [28] C. Berge, *Graphs and Hypergraphs*. American Elsevier Pub. Co, 1973.
- [29] X. Ouyard, “Hypergraphs: an introduction and review,” *arXiv:2002.05014*, 2020.
- [30] I. Kapovich and N. Benakli, “Boundaries of hyperbolic groups,” *arXiv preprint math/0202286*, 2002.
- [31] F. Ji, W. Tang, and W. P. Tay, “On the properties of Gromov matrices and their applications in network inference,” *IEEE Trans. Signal Process.*, vol. 67, no. 10, pp. 2624 – 2638, May 2019.
- [32] B. Klimt and Y. Yang, “Introducing the enron corpus.” in *CEAS*, 2004.
- [33] P. Sen, G. Namata, M. Bilgic, L. Getoor, B. Galligher, and T. Eliassi-Rad, “Collective classification in network data,” *AI mag.*, vol. 29, no. 3, p. 93, 2008.